Environ. Sci. Technol. **2004**, *38,* 5598−5603

Use of Ferrocenyl Surfactants of Varying Chain Lengths To Study Electron Transfer Reactions in Native Montmorillonite Clay

CARLA SWEARINGEN,* JUN WU,‡ JOSEPH STUCKI,‡ AND ALANAH FITCH§

Department of Chemistry, Loyola University Chicago, 6525 North Sheridan Road, Chicago, Illinois 60626, and Department of Natural Resources and Environmental Sciences, University of Illinois, Urbana−Champaign, Urbana, Illinois 61801

A series of ferrocenyl surfactants was tested as model compounds to study electron transfer reactions involving structural Fe(III) in clay minerals. The surfactants contain trimethylammonium headgroups, ferrocene tail groups, and intervening hydrocarbon chain lengths of one, six, or 11 carbons. Two factors considered to be decisive for electron transfer were addressed: (1) physical access of the surfactant ferrocene to the reactive sites through hexagonal holes in the clay lattice by X-ray diffraction (XRD) and small-angle X-ray scattering (SAXS) and (2) thermodynamic favorability of the overall oxidation/reduction reaction based on experimentally determined oxidation/reduction potentials. In suspensions of clay with the longer chain surfactants, (ferrocenylhexyl)trimethylammonim ($FHTMA^+$) and (ferrocenylundecyl)trimethylammonium ($FUTMA^+$), where electron transfer may be expected to be favored by both factors, physical accessibility, and thermodynamic favorability, ferroecene oxidation was observed by diffuse reflectance infrared spectroscopy (DRIFT), ultraviolet−visible spectroscopy (UV−vis), and visual color changes. In contrast, the shorter chain length surfactant, (ferrocenylmethyl)trimethylammonium ($FMTMA^+$), did not participate in electron transfer with the clay, as substantiated by UV−vis and no visible color changes. Rigid conformation and/or higher oxidation/reduction potential than clay Fe can account for the lack of reaction. The utility and limitations of using these surfactants as model compounds is discussed.

Introduction

Electron transfer reactions utilizing clays as tailorable templates and/or actual oxidation/reduction reactants due to electrochemically active metal sites within the clay structure are poorly understood. Because clays are ubiquitous; have a large surface area; have the ability to exchange cations; come in a variety of sizes, shapes, layer charges, and elemental composition; and are low cost, they represent an underutilized technology. In the environment, clays are known to be an active mineral component of soils and subsequently influence greatly the movement of cations, anions, metals, and organics (*1*). Furthermore, the movement and sorption of cations is influenced to the greatest extent in the environment by smectite clays (*2*).

There is overwhelming evidence that Fe substitution sites within clay lattices are not inert, and Fe is often available to participate in oxidation/reduction reactions. In particular, Fe substitution sites within smectites have been a topic of study because of the important role smectites play in the environment. Among the most investigated compounds used to effect reduction of structural Fe(III) to Fe(II) in clays are benzidine and dithionite, and these spontaneous oxidation/reduction reactions are often accompanied by vibrant color changes (*3*). Various other physical and chemical properties of clays are, in part, determined by Fe concentration and oxidation state. For example, the Fe oxidation state influences specific surface area (*4*) and swelling behavior. Reduction of Fe(III) to Fe(II) decreases swelling, an observation noted as early as 1953 by Foster with a simple graduated cylinder experiment (*5*). In turn, this swelling behavior can affect transport of nutrients and pollutants in the environment (*2*, *6*).

An important property of reduced clays that can lead to interesting engineering applications is their ability to reductively transform contaminants in situ. Toxic substances such as tricholorethane (*7*), pentachloroethane (*8*), and chromium (*9*) can be reduced to less toxic states via electron donation within soil matrixes. Intercalating and nonintercalating nitroaromatics have been used to probe the effects of basal versus edge surface oxidation/reduction reactions, with the finding that clay structural Fe was able to reduce nitroaromatics (*10*). In a field study, researchers at the Hanford site in Washington were able to reduce the amount of Cr(VI) in the water supply from 1 ppm to below detection limits of 7−8 ppb (*11*−*13*). In this process, Fe(III) was first reduced to Fe(II) with use of sodium dithionite pumped into wells. The reduced Fe then served as a source of electrons to reduce Cr(VI) to Cr(III), a much less toxic and less soluble form of Cr. In some of the examples listed previously, Fe oxides present on the surface may partially account for the desired electrochemical activity. However, since the function of structural Fe has not been extensively elucidated, its role in electrochemical reactions warrants further study. Previous studies have mainly focused on single probes, whereas this one encompasses a series of homologous compounds.

Determination of conditions when electronic transfer takes place in clay structural Fe can lead to a better general knowledge of Fe activity in natural silicates. To this end, a series of ferrocenyl surfactants of varying chain lengths was employed as intercalants. They consist of (ferrocenylmethyl)-trimethylammonium ($FMTMA^+$) chloride, (ferrocenylhexyl)-trimethylammonim ($FHTMA^+$) bromide, and (ferrocenylundecyl)trimethylammonium ($FUTMA^+$) bromide, as shown in Figure 1A. The chemistry of $FMTMA^+$ (*14*) and $FUTMA^+$ (*15*−*23*) has been reviewed extensively in the literature. Within each compound, an ammonium headgroup acts as an anchor to the clay and ferrocene as the electroactive tail group. The variable in these compounds is the hydrocarbon chain length (one, six, or 11 carbons), where chain length not only determines the possible accessibility of the ferrocene group to hexagonal holes of the clay but also changes the electrochemical potential of the ferrocene. In this study, the hypotheses are addressed that electron transfer from Fe(II) in the ferrocene group to Fe(III) in the clay is possible if (1) the ferrocene group is keyed into the hexagonal hole (i.e., the two reacting sites are held in close proximity to each

* Corresponding author e-mail: cswearin@uiuc.edu.
‡ Department of Natural Resources and Environmental Sciences, University of Illinois.
§ Loyola University Chicago.

10.1021/es030645+ CCC: $27.50
Published on Web 09/29/2004

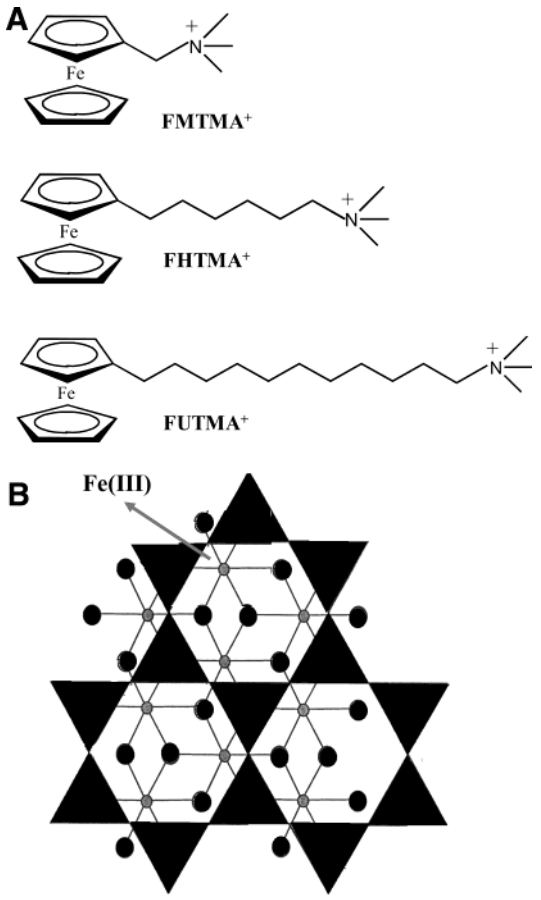

FIGURE 1. (A) Ferrocenyl surfactants where FMTMA$^+$ is (ferrocenylmethyl)trimethylammonium, FHTMA$^+$ is (ferrocenylhexyl)-trimethylammonium, and FUTMA$^+$ is (ferrocenylundecyl)trimethylammonium. (B) Basic tetrahedral clay layer with hexagonal holes on top. Access to Fe(III) is shown in the underlying layer.

other) and (2) the oxidation/reduction potential is favorable for the overall oxidation/reduction reaction.

Previous X-ray diffraction (XRD) data have shown that the trimethylammounium headgroups of similar surfactants are not only electrostatically attracted to the clay but are positioned inside the hexagonal cavities of the clay (*24*), which have a size of 5 Å (Figure 1b). On the basis of this size, ferrocene was chosen as the electroactive portion of the surfactant because it has an interring distance of 3.3 Å and an estimated cubic shape of 4.1 Å (*25*). On the basis of these estimates, ferrocene would be able to fit into these cavities. Assuming the trimethylammonium headgroup is anchored in the clay, the ability of ferrocene to insert into these cavities is based on conformation of the intervening hydrocarbon chain. The chain length of surfactants has a significant effect on the orientation at the clay surface (*26*). Gallardo et al. found that the short chain FMTMA$^+$ has a vertical orientation at the surface of water (*16*). In contrast, the ferrocene in the longer and more flexible FUTMA$^+$ chains is not constrained in this way. These chains may bend over, allowing both the trimethylamine and the ferrocene to interact with the surface of water in a direct manner (*16*). On the basis of the fact that chain length played a major role in conformation at the surface of water, it was predicted that it would also play a large role in conformation at a clay surface.

The ability of the ferrocene group to directly insert into the hexagonal holes is expected to facilitate electron-transfer reactions with clay Fe. In a similar study, Okuno and Matsubayashi demonstrated that the Fe in a series of ferrocenyl surfactants oxidized when intercalated into synthetic vanadium clay with subsequent reduction of vanadium (*27*). This oxidation, however, only occurred in compounds in which the ferrocenes had direct access to the vanadium.

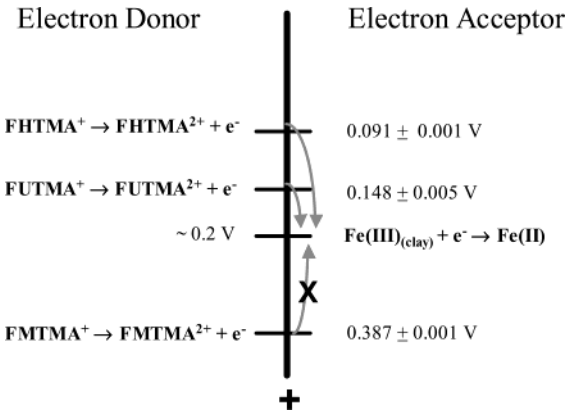

FIGURE 2. Energy scheme for possible oxidation/reduction reactions of ferrocenyl surfactants with sturctural Fe(III) in clay. Because energy is depicted going from negative to positive, a thermodynamically spontaneous reaction involves electrons flowing down the scheme. Potentials measured from cyclic voltammograms and standard deviation from at least three measurements.

As stated previously, direct access to structural Fe is not the only factor in ferrocene's ability to donate electrons. The electron transfer reaction must also be thermodynamically favorable. Figure 2 shows the series of ferrocenyl surfactants and their experimentally determined oxidation/reduction potentials (*28*). It is evident that the ferrocene tail group is strongly affected by the nature and length of the attached chain (*29*). In the case of FMTMA$^+$, the relatively high reduction potential is due to the electron withdrawing capabilities of the trimethylammonium group. Conversely, if the ferrocene group is insulated from the trimethylammonium group by a longer alkyl chain, the reduction potential of ferrocene is most strongly influenced by the electron donating capabilities of the long hydrocarbon chain, as in FHTMA$^+$ and FUTMA$^+$. Therefore, the choice of ferrocenyl surfactants with various chain lengths gives both a range of potentials and a range of possible conformations. The objective of this study is to intercalate these ferrocene-containing surfactants into native montmorillonite suspensions in an effort to elucidate factors involved in electron transfer between the ferrocene and clay Fe(III).

Experimental Procedures

All chemicals were used as received from Aldrich unless otherwise specified. FMTMA$^+$ was obtained from Lancaster in the iodide form and exchanged to the chloride form on an ion-exchange resin (*30*). Synthesis of FUTMA$^+$ followed the method of Saji et al. (*23*). Briefly, 11-bromoundecanoic acid was converted to the acyl bromide by treatment with oxalyl chloride. 11-Bromoundecanoyl chloride was reacted with ferrocene via a Friedel−Crafts acylation with anhydrous aluminum chloride as catalyst. The resulting (11-bromoundecanoyl)ferrocene was converted to (11-bromoundecyl)-ferrocene with the Clemmenson Reduction. Displacement of the bromine with trimethylamine afforded the desired product. ^{1}H nuclear magnetic resonance spectroscopy (NMR) and mass spectrometry (MS) confirmed the structure of the product. FHTMA$^+$ was synthesized in a manner similar to FUTMA$^+$, utilizing 6-bromohexanoic acid as the starting material.

Clays were obtained from the Source Clay Repository (Columbia, MO) and purified as described elsewhere (*31*). Standard Wyoming montmorillonite (SWy-1) with the formula $(Al_{2.88}Fe_{0.68}Mg_{0.47})(Si_{7.7}Al_{0.29})O_{20}(OH)_4$ and a cation ex-

change capacity (CEC) of 76.4 meq/100 g (*32*) and hectorite (SHCa) with the formula $(Mg_{5.34}Li_{0.66})Si_8O_{20}(OH)_4$ and CEC of 43.9 meq/100 g (*32*) suspensions were made from 10 g/L purified Na-exchanged clay. Suspensions were made by mixing surfactant at an amount of 33% of the CEC of the clay (0.25 M for SWy-1 and 0.14 M for SHCa). (This percentage was chosen to maximize oxidation/reduction reactions and minimize sample flocculation.) Samples were vortexed for >10 min to ensure complete mixing. Unless otherwise noted, pH and temperature were not externally controlled.

To measure interlayer spacings of clays, X-ray diffraction (XRD) and small-angle X-ray scattering (SAXS) were performed. 33% suspensions were prepared and pipetted onto a glass slide. After drying, interlayer spacings were determined on a Siemens D-500 Diffractometer containing a Cu radiation source. SAXS analysis was performed at the Advanced Photon Source at Argonne National Laboratories. 33% suspensions of the samples were transferred to 1.5 mm capillary tubes for analysis.

Oxidation/reduction potentials for the three ferrocenyl surfactants were experimentally determined by cyclic voltammetry with clay-modified electrodes, described previously (*28*, *33*−*35*). Briefly, a 1 μL aliquot of a 10 g/L SWy-1 suspension was applied to a Pt electrode and spun at 800 rpm for 20 min. The clay-modified electrode was preswollen in 0.1 M NaCl for 10 min. Cyclic voltammetry was then performed in 0.4 mM surfactant in 0.1 M NaCl until steady state was achieved.

For diffuse reflectance infrared spectroscopy (DRIFT) spectra, the surfactant was added at a rate of 33% of CEC to 30 mg of clay in 3 mL of water and suspended for two weeks. The suspension was dried in a hood and scraped from the container and dried in a vacuum, and a spectra was obtained on a Nicolet Nexus 870 Fourier Transform-Infrared Spectrometer (FT-IR).

UV−vis spectra were obtained on a Varian Cary 5E UV−vis spectrophotometer with a magnetic stirrer in the cuvette to prevent settling of the flocculants. SWy-1 samples were diluted with 0.2 M citrate-bicarbonate buffer to maintain a pH of 8.4. Surfactant was added at a rate of 33% of CEC. Reduced clays were reduced with sodium dithionite (5 times dithionite to clay) at 70 °C under $N_{2(g)}$, as described previously (*4*, *28*, *36*) and were washed and centrifuged three times before being suspended in surfactant. Reoxidation was effected by bubbling H_2O-saturated $O_{2(g)}$ through the suspensions. For reference spectra, ferrocene was dissolved in methanol, and oxidation was effected by adding an excess of ceric (IV) sulfate.

Results and Discussion

As stated in the Introduction, electron transfer between clay structural Fe and ferrocenyl Fe is expected to occur if the two are in close proximity and there is an electrochemical potential match. To estimate proximity, XRD was previously used to look at the interlayer spacing of SWy-1 when intercalated with the three surfactants (*28*). Briefly, suspensions of SWy-1 with 33% $FMTMA^+$ were found to have larger basal spacings than either $FHTMA^+$ or $FUTMA^+$ suspensions (4.9 Å vs 4.83 and 4.78 Å, respectively.) Incidentally, since the spacing of SWy-1 by itself (1.72 Å) is much smaller, this clearly indicates that the surfactants are intercalated into the interlayer region. In addition, the estimated chain lengths of the surfactants when fully extended are 1.5, 6.4, and 12.7 Å, respectively, making it impossible for the $FHTMA^+$ and $FUTMA^+$ chains to be fully extended in the clay interlayer. A limitation of XRD is that the samples must be dried before analysis, so the interlayer spacings obtained may or may not reflect the actual spacings in solution. However, the same trend occurred SAXS, which was used to determine interlayer spacings of wet samples. Aqueous suspensions of SWy-1 with 33% $FMTMA^+$ gave spacings of 6.5 Å, while $FHTMA^+$ and $FUTMA^+$ were 5.8 and 5.9 Å, respectively. While it is difficult to draw absolute conclusions about conformations of the three surfactants, it is evident that the longer chains are not vertically oriented to the clay, allowing for the possibility for ferrocene to interact directly with the clay surfaces. On the basis of the size of the smaller chain, this appears to be much less likely for $FMTMA^+$.

TABLE 1. Observed Major IR Bands in cm^{-1} [a]

ferrocene	$FUTMA^+$	ferrocenium	$FUTMA^+$/SWy-1	assignment
3077	3096	3108	3118	C-H stretch
1410	1408	1421	1418	C-C stretch
1100	1103	1116	1112	C-C stretch
1005	998	1017		C-H deform.
855	856	860		C-H
820	819	805		C-H
492		501	493	ring tilt
478	485	423	419	Fe-Cp stretch

[a] When not listed, bands are obscured and could not be determined. $FUTMA^+$ present at 33% CEC of 10 g/L SWy-1.

According to the XRD and SAXS data, ferrocene in the longer chains has the potential to access Fe present in the clay, but there must also be an electrochemical potential match. The oxidation/reduction potential of the structural Fe (III) in clay is estimated to be 0.2 V vs a saturated calomel reference electrode (SCE) (*37*), and the oxidation/reduction potentials of the three surfactants were experimentally determined by cyclic voltammetry. A reduction potential of 0.2 V would allow $FHTMA^+$ and $FUTMA^+$, but not $FMTMA^+$, to be electron donors to the clay (see Figure 2). On the basis of both orientation and potentials observed, it was predicted that the ferrocene in $FHTMA^+$ and $FUTMA^+$ would be oxidized in the suspension with SWy-1, but the ferrocene in $FMTMA^+$ would not react.

Oxidation of the ferrocene within the clay/surfactant suspension was observed for SWy-1 composites of $FHTMA^+$ and $FUTMA^+$ but was not observed for SWy-1 composites of $FMTMA^+$, as anticipated. Oxidation in the longer chain surfactants was easily observed by eye as the solution turned from yellow to green to blue/gray. Neutral ferrocene in solution is yellow, and positively charged ferrocenium is blue, giving rise to the observed color changes. Conversely, oxidation of ferrocene with the one carbon chain surfactant did not occur when placed in suspension with SWy-1 under any conditions, as evidenced by a lack of color change.

Oxidation of the ferrocene moiety was also confirmed by both DRIFT and UV−vis. As seen in Table 1, the DRIFT band shifts for solution phase $FUTMA^+$ to $FUTMA^+$ in the SWy-1 composite mirror the shifts from ferrocene to ferrocenium (*38*). Most notably, the band shifts for the iron-cyclopentadienyl ring bonds are diagnostic of iron oxidation state. Upon removal of a bonding electron from Fe, there is a decrease in the strength of the Fe-cyclopentadienyl ring bond, causing the observed shift from 478 to 423 cm^{-1} for ferrocene to ferrocenium (*39*, *40*). Similarly, vibrations of $FUTMA^+$ shifted from 485 to 419 cm^{-1} in the presence of SWy-1 and confirmed that the major product formed was the oxidized surfactant.

UV−vis spectra of suspensions of surfactant and clay were also used to substantiate oxidation of the ferrocene in $FHTMA^+$ and $FUTMA^+$ in SWy-1 suspensions. Both clay and ferrocene oxidation states can theoretically be monitored by UV−vis. The Si−O and Al−O lattice of clays do not absorb light in the UV−vis region, so that the only peaks that occur are due to transition metal cations, most notably Fe(III) (*41*). However, in practice, because of the large background due to clay particle scattering, the oxidation state of the ferrocene is more easily tracked.

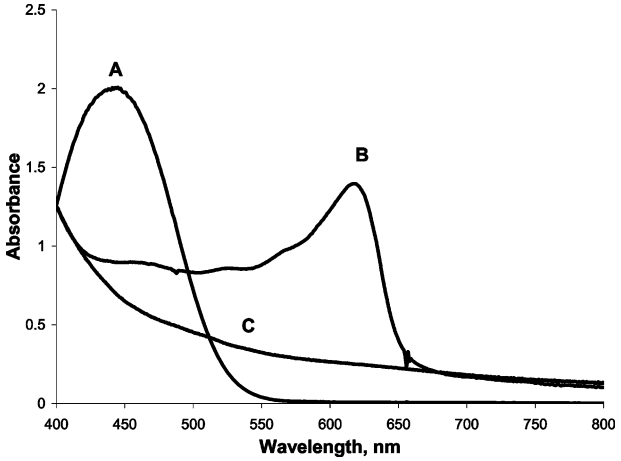

FIGURE 3. (A) UV−vis spectrum of ferrocene in methanol. (B) UV−vis spectrum of ferrocenium prepared by chemically oxidizing ferrocene with ceric(IV) sulfate. (C) UV−vis spectrum of SWy-1 in water.

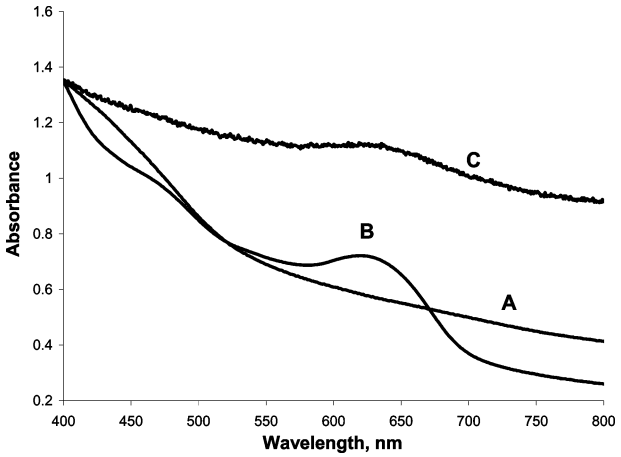

FIGURE 4. (A) UV−vis spectrum of FMTMA$^+$/SWy-1 suspension. (B) UV−vis spectrum of FHTMA$^+$/SWy-1 suspension. (C) UV−vis spectrum of FUTMA$^+$/ SWy-1 suspension.

TABLE 2. UV−Vis λ_{max} for Reduced and Oxidized Surfactants[a]

	λ_{max} (reduced)	λ_{max} (oxidized)
FMTMA$^+$	417	629
FHTMA$^+$	437	627
FUTMA$^+$	439	628
ferrocene	445	619

[a] Chemical oxidation was achieved by mixing with Ce(IV).

For reference, a UV−vis spectrum was taken of neutral ferrocene in methanol. As seen in Figure 3, the maximum absorbance occurs at 445 nm. When oxidized, the major absorbance peak shifts to 619 nm (*29*, *42*). Table 2 lists the experimentally determined λ_{max} associated with the reduced and oxidized forms of the three surfactants in aqueous solutions. The UV−vis spectrum of an SWy-1/water suspension is also shown in Figure 3. It reveals that there are no peaks between 400 and 650 nm, aside from the high background scattering, allowing this region to be used for determination of ferrocene oxidation state in the clay.

Figure 4 shows UV−vis spectra of the ferrocenyl surfactants in suspension with SWy-1. For FMTMA$^+$, there is a broad shoulder centered around 450 nm and no discernible peaks in the 600−700 nm region, implying that the ferrocene in FMTMA$^+$ is in the original, reduced state. The UV−vis spectrum of a suspension of FHTMA$^+$/SWy-1 reveals a defined peak at 620 nm and a much smaller, broader peak centered around 460 nm, indicating significant, but incomplete, ferrocene oxidation. Likewise, the UV−vis spectrum of an FUTMA$^+$/SWy-1 suspension reveals a peak centered at 625 nm. The UV−vis data demonstrate that the ferrocenes in FHTMA$^+$ and FUTMA$^+$ in suspension with SWy-1 are oxidized to ferrocenium, while the ferrocene in FMTMA$^+$ remains neutral under similar conditions.

It has previously been shown that the presence of oxygen can account for oxidation of ferrocene (*28*). The mechanism of ferrocene oxidation via oxygen requires an acidic environment to protonate the Fe(II) before oxygen attack (*43*, *44*). On the basis of this evidence, it might be assumed that the purpose of the clay is simply to provide an acidic interlayer environment for ferrocene oxidation to occur. However, based on what is known about the oxidizing ability of clay structural Fe(III), it was postulated that clay lattice Fe(III) is a factor in oxidation. To separate out the effects of the two processes (acidic catalysis by oxygen versus clay structural Fe(III) electron donation), several experiments were performed.

Because oxidation via $O_{2(g)}$ requires an acidic environment, an experiment was performed with where the pH of the solution was altered. When FHTMA$^+$/SWy-1 and FUTMA$^+$/SWy-1 suspensions are prepared in 0.2 M citrate-bicarbonate buffer (pH ~8.4), oxidation still takes place. Within a few hours after preparation, the FMTMA$^+$/SWy-1 suspension remains yellow, while the FHTMA$^+$/SWy-1 suspension begins to turn blue/green and the FUTMA$^+$/SWy-1 suspension begins to turn blue/gray. The lack of oxidation of FMTMA$^+$ can be explained by the fact that the oxidation reaction is less thermodynamically favorable than for the longer chain surfactants (*28*). After several days, these colors are intensified. In neat solutions (clay-free) in citrate-bicarbonate buffer, FHTMA$^+$ and FUTMA$^+$ do not show oxidation of the ferrocene moiety.

A second method of preventing the acid-facilitated $O_{2(g)}$ oxidation reaction was to directly eliminate $O_{2(g)}$. Experiments with SWy-1 performed in the absence of oxygen show that oxidation of the ferrocene still occurs. When FHTMA$^+$/SWy-1 and FUTMA$^+$/SWy-1 were prepared with $N_{2(g)}$-purged solutions in an $N_{2(g)}$-purged glovebag, oxidation begins to occur immediately, as observed by the color change to light green. After 48 h, a blue/gray color has developed, revealing significant oxidation.

The fact that removal of conditions in which $O_{2(g)}$ would cause oxidation do not, in fact, prevent oxidation of ferrocene in FHTMA$^+$ and FUTMA$^+$ in SWy-1 suspensions provides indirect evidence that structural Fe(III) in the clay is participating in the electron-transfer reaction. Further evidence of this relationship was provided by altering the Fe(III) content of the clay.

Hectorite (SHCa) clay has no Fe(III) present in the crystal lattice. Therefore, suspensions of FHTMA$^+$ and FUTMA$^+$ in SHCa made in the absence of oxygen are not expected to result in oxidation. Preparation of these FHTMA$^+$ and FUTMA$^+$ suspensions in the $N_{2(g)}$-purged glovebag gave the expected results. Even after 10 days, both suspensions remained yellow, indicating that no ferrocene oxidation had occurred. When placed outside the glovebag, these suspensions turned blue/gray after only 1 day of exposure to air.

More quantifiable evidence of the role of structural Fe(III) in these oxidation/ reduction reactions was provided by a series of UV−vis experiments, in which the clay type was held constant and the oxidation state of the Fe(III) altered. Clay suspensions were prepared under four different conditions: (a) SWy-1 in air, (b) SWy-1 under $N_{2(g)}$ atmosphere, (c) reduced SWy-1 under $N_{2(g)}$, and (d) reduced/reoxidized SWy-1 in air. Each sample reacted with the three surfactants. The reduced clay samples have the lattice Fe(III) reduced to

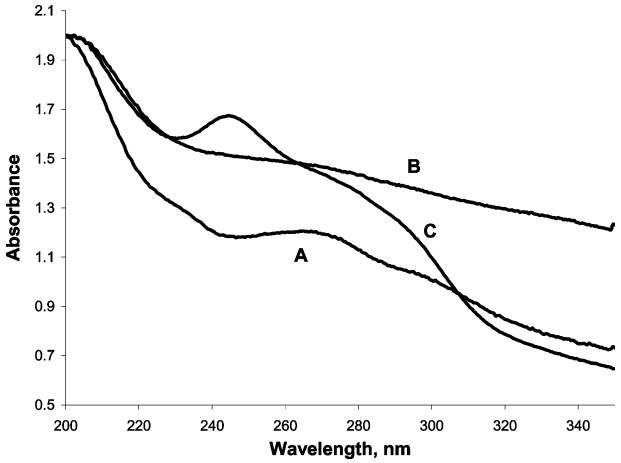

FIGURE 5. UV−vis of (A) unaltered SWy-1, (B) reduced SWy-1, and (C) reduced/ reoxidized SWy-1.

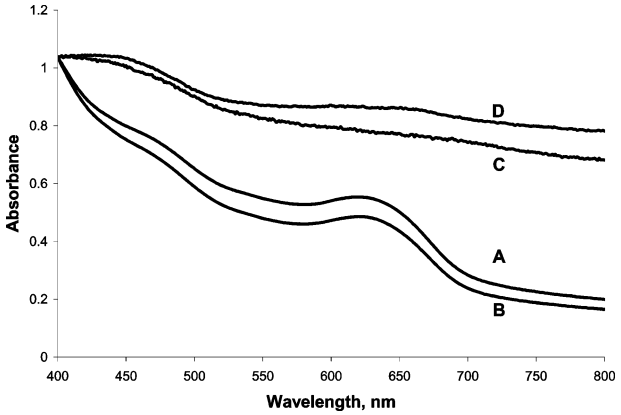

FIGURE 6. UV−vis spectra of FHTMA$^+$/SWy-1 suspensions under different conditions: (A) unaltered SWy-1 in air, (B) unaltered SWy-1 in $N_{2(g)}$, (C) reduced SWy-1 in $N_{2(g)}$, and (D) reduced/reoxidized SWy-1 in air.

Fe(II) by chemical reduction with $Na_2S_2O_{4(aq)}$. The reduced/ reoxizidized samples were first reduced and then exposed to $O_{2(g)}$ for reoxidation. Reduction and reoxidation of structural Fe(III) can be confirmed by evaluating the 200−300 nm region of the UV−vis spectrum. Montmorillonites typically show a peak in 240−245 range, attributed to charge transfer between Fe(III)-oxygen ligands (*41*). Upon reduction of Fe(III) to Fe(II), this band disappears and is accompanied by loss of structural hydroxide (*36*, *45*, *46*). Figure 5 shows that the unaltered SWy-1 suspension has a broad peak centered at 265 nm that disappears to a flat line upon reduction of structural Fe(III). When reoxidized, the peak returns but is shifted to 245 nm, signaling that the original structure is not completely restored. Although the exact structure after reoxidation is not known, it can be hypothesized based on the shift to shorter wavelengths that the bond length for Fe(III)−oxygen is shorter than in the unaltered sample (*41*, *47*).

Figure 6 shows UV−vis spectra of FHTMA$^+$ samples under the four clay conditions. The unaltered SWy-1 suspension reveals a small peak at 460 nm and a sharper peak at 630 nm. The peak at 630 nm illustrates that the ferrocene is in the oxidized state, substantiated visually by a blue color. When the same samples are prepared under anoxic conditions, the UV−vis spectrum has the same features as the sample prepared under air, revealing that even without the presence of $O_{2(g)}$, oxidation of the ferrocene takes place. A suspension produced with reduced SWy-1 retains a yellow color and exhibits no peak at 630 nm. This indicates that ferrocene remains in the neutral state when both $O_{2(g)}$ and Fe(III) are

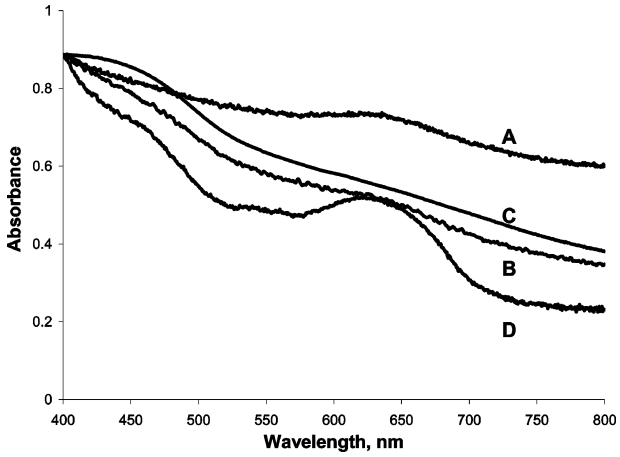

FIGURE 7. UV−vis spectra of FUTMA$^+$/SWy-1 suspensions under different conditions: (A) unaltered SWy-1 in air, (B) unaltered SWy-1 in $N_{2(g)}$, (C) reduced SWy-1 in $N_{2(g)}$, and (D) reduced/reoxidized SWy-1 in air.

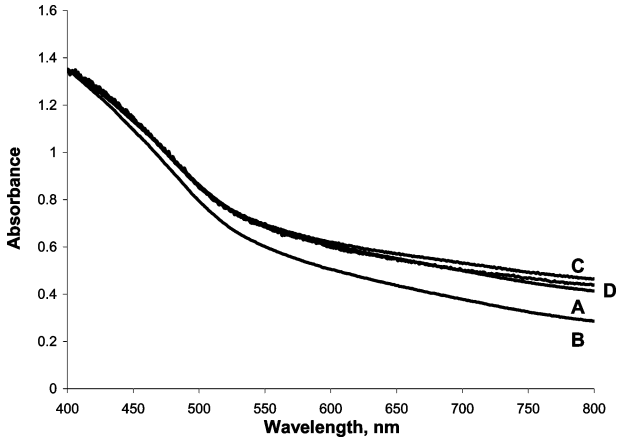

FIGURE 8. UV−vis spectra of FMTMA$^+$/SWy-1 suspensions under different conditions: (A) unaltered SWy-1 in air, (B) unaltered SWy-1 in $N_{2(g)}$, (C) reduced SWy-1 in $N_{2(g)}$, and (D) reduced/reoxidized SWy-1 in air.

absent. If the SWy-1 is first reduced and then reoxidized, the peak at 630 nm returns. Suspensions prepared with FUTMA$^+$ mimic those of FHTMA$^+$, as revealed by similar UV−vis spectra in Figure 7. These UV−vis experiments reveal two things. First, while $O_{2(g)}$ can account for oxidation of ferrocene in clay, even when this source is removed, oxidation via structural Fe still occurs. Second, if both sources of oxidation are removed ($O_{2(g)}$ and structural Fe(III)), ferrocene oxidation does not occur, demonstrating that these two factors alone caused oxidation in these experiments.

As a control, similar experiments were performed for FMTMA$^+$. On the basis of the consideration of both potential and structure, this compound was not expected to undergo any oxidation/reduction reactions. As can be seen in Figure 8, UV−vis spectra of FMTMA$^+$ samples mixed with SWy-1 under all four conditions stated previously show the same basic feature. The broad peak at 450 nm reveals that the ferrocene in FMTMA$^+$ remains in the reduced state, as expected. Ferrocene oxidation is prevented by surfactant conformation and/or surfactant electrochemical potential. Table 3 provides a summary of the maximum wavelength and color observed for all of the conditions.

In summary, both oxygen and clay structural Fe(III) can result in oxidation of ferrocene in FHTMA$^+$ and FUTMA$^+$ in suspension with SWy-1. Similarly, Furukawa and Brindley found that the color change of benzidine on montmorillonite

TABLE 3. UV−Vis λ_{max} and Color Observed for Suspensions of $FMTMA^+$, $FHTMA^+$, $FUTMA^+$, and SWy-1 under Four Different Treatment Conditions

compound	SWy-1 treatment	λ_{max} (nm)	color
$FMTMA^+$	unaltered (air)	450	yellow
	unaltered ($N_{2(g)}$)	450	yellow
	reduced	450	yellow
	reduced/reoxidized	450	yellow
$FHTMA^+$	unaltered (air)	630	green
	unaltered ($N_{2(g)}$)	630	green
	reduced	450	yellow
	reduced/reoxidized	630	yellow
$FUTMA^+$	unaltered (air)	630	green
	unaltered ($N_{2(g)}$)	630	green
	reduced	450	yellow
	reduced/reoxidized	630	green

occurred by these same two processes (*48*). The individual contribution of each is, however, tough to quantitate from the methods utilized in this paper. An additional experimental limitation is the fact that the effect of conformation and electrochemical potential of the three surfactants is difficult to separate. $FMTMA^+$ is not expected to undergo electron transfer with clay structural Fe based on both conformation and electrochemical potential arguments. It is, therefore, impossible to determine which is preventing electron transfer. Future work could include utilizing a similarly rigid ferrocenyl molecule with an electrochemical potential that is lower than clay structural Fe. The difficulty in this suggestion is trying to keep the basic structure of the molecules the same for comparison purposes, and a similar structure explains the rationale for the choice of surfactants utilized in this work.

The fact that $FHTMA^+$ and $FUTMA^+$ both participate in electrochemical reactions, as anticipated, is evidence that the correct factors for electron transfer were considered. It also demonstrates that electron transfer with Fe in native montmorillonite is possible if there is physical access and thermodynamic incentive. Oxidation/reduction studies addressing intercalates in clay deal with an inherently complicated system, involving acid/base reactions, potential matches, direct access to Fe(III), and the presence of other oxidants/reductants (among other possible unknowns). These factors become even more convoluted when the desire is to move from the laboratory to the natural environment. However, due to the relative abundance of clays in the environment, their potential for participation in in situ remediation warrants further scientific investigation.

Acknowledgments

Dan McAlister is acknowledged for acquisition of DRIFT data. Susan Macha is acknowledged for SAXS data. C.S. thanks Steve Guggenheim for XRD instrumentation use. C.S. acknowledges a Loyola University Chicago GAANN Fellowship and National P.E.O. Scholar Award.

Literature Cited

(1) Miller, R. W.; Gardiner, D. T. *Soils in Our Environment*; Prentice Hall: Upper Saddle River, NJ, 2001.
(2) Stucki, J. W.; Wu, J.; Gan, H.; Komadel, P.; Banin, A. *Clays Clay Miner.* **2000**, *48*, 290−298.
(3) Theng, B. K. G. *Clays Clay Miner.* **1971**, *19*, 383−390.
(4) Lear, P. R.; Stucki, J. W. *Clays Clay Miner.* **1985**, *33*, 539−545.
(5) Foster, M. D. *Am. Mineral.* **1953**, *38*, 994−1006.
(6) Stucki, J. W.; Low, P. F.; Roth, C. B.; Golden, D. C. *Clays Clay Miner.* **1984**, *32*, 357−362.
(7) Cervini-Silva, J.; Larson, R. A.; Wu, J.; Stucki, J. W. *Environ. Sci. Technol.* **2001**, *35*, 805−809.
(8) Cervini-Silva, J.; Wu, J.; Stucki, J. W.; Larson, R. A. *Clays Clay Miner.* **2000**, *48*, 132−138.
(9) Brigatti, M. F.; Lugli, C.; Cibin, G.; Marcelli, A.; Guili, G.; Paris, E.; Mottana, A.; Wu, Z. *Clays Clay Miner.* **2000**, *48*, 272−281.
(10) Hofstetter, T. B.; Schwarzenbach, R. P.; Haderlein, S. B. *Environ. Sci. Technol.* **2003**, *37*, 519−528.
(11) Williams, M. D.; Vermeul, V. R.; Szecsody, J. E.; Fruchter, J. S. *PNNL-13349: 100-D area in situ redox treatability test for chromate-contaminated groundwater*; Pacific Northwest National Laboratory: Richland, WA, 2000.
(12) Chilakapati, A.; Williams, M.; Yabusaki, S.; Cole, C.; Szecsody, J. *Environ. Sci. Technol.* **2000**, *34*, 5215−5221.
(13) Fruchter, J. S. *Environ. Sci. Technol.* **2002**, *36*, 464A−472A.
(14) Takehara, K.; Takemura, H. *Bull. Chem. Soc. Jpn.* **1995**, *68*, 1289−1296.
(15) Yokoyama, S.; Kurata, H.; Harima, Y.; Yamashita, K.; Hoshino, K.; Kokado, H. *Chem. Lett.* **1991**, *3*, 441−444.
(16) Gallardo, B. S.; Metcalfe, K. L.; Abbott, N. L. *Langmuir* **1996**, *12*, 4116−4124.
(17) Gallardo, B. S.; Hwa, M. J.; Abbott, N. L. *Langmuir* **1995**, *11*, 4209−4212.
(18) Saji, T.; Hoshino, K.; Aoyagui, S. *J. Chem. Soc. Chem. Commun.* **1985**, *107*, 865−866.
(19) Fraser, D. M.; Zakeeruddin, S. M.; Grätzel, M. *Biochim. Biophys. Acta* **1992**, *1099*, 91−101.
(20) Rosslee, C. A.; Abbott, N. L. *Anal. Chem.* **2001**, *73*, 4808−4814.
(21) Hoshino, K.; Saji, T. *J. Am. Chem. Soc.* **1987**, *109*, 5881−5883.
(22) Hoshino, K.; Suga, K.; Saji, T. *Chem. Lett.* **1986**, *6*, 979−982.
(23) Saji, T.; Hoshino, K.; Ishii, Y.; Goto, M. *J. Am. Chem. Soc.* **1991**, *113*, 450−456.
(24) Martin-Rubi, J. A.; Rausell-Colom, J. A.; Serratosa, J. M. *Clays Clay Miner.* **1974**, *22*, 87−90.
(25) Therias, S.; Lacroix, B.; Schöllhorn, B.; Mousty, C.; Palvadeau, P. *J. Electroanal. Chem.* **1998**, *454*, 91−97.
(26) Laby, R. H.; Walker, G. F. *J. Phys. Chem.* **1970**, *74*, 2369−2373.
(27) Okuno, S.; Matsubayashi, G.-E. *J. Chem. Soc. Dalton Trans.* **1992**, *16*, 2441−2444.
(28) Swearingen, C. B. Rational design of novel electroactive clay nanocomposites modified with ferrocenyl surfactants of varying chain lengths. Ph.D. Dissertation, Loyola University, Chicago, 2002.
(29) de Santis, G.; Fabrizzi, L.; Licchelli, M.; Monichino, A.; Pallavicini, P. *J. Chem. Soc. Dalton Trans.* **1992**, *14*, 2219−2224.
(30) Macha, S. Transport control in thin clay films: Clay-modified electrode studies of mixed electrolyte systems and intercalated electroactive surfactants. Ph.D. Dissertation, Loyola University, Chicago, 2001.
(31) Lee, S. A.; Fitch, A. *J. Phys. Chem.* **1990**, *94*, 4998−5004.
(32) Newman, A. C. D., Ed. *Chemistry of Clays and Clay Minerals*; John Wiley and Sons: New York, 1987.
(33) Ghosh, P. K.; Bard, A. J. *J. Am. Chem. Soc.* **1983**, *105*, 5691−5693.
(34) Subramanian, P.; Fitch, A. *Environ. Sci. Technol.* **1992**, *26*, 1775−1779.
(35) Fitch, A. *Clays Clay Miner.* **1990**, *38*, 391−400.
(36) Komadel, P.; Madejova, J.; Stucki, J. W. *Clays Clay Miner.* **1995**, *43*, 105−110.
(37) Amonette, J. E. *Clay Minerals Society Workshop Lecture Series*; Fitch, A., Ed.; Clay Minerals Society: Chicago, 2003; Vol. 10.
(38) Nakamoto, K. *Infrared and Raman Spectra of Coordination Compounds*; John Wiley and Sons: New York, 1986.
(39) Haaland, A. *Acc. Chem. Res.* **1979**, *12*, 415−422.
(40) Pavlik, I.; Klikorka, J. *Coll. Czech. Chem. Commun.* **1965**, *30*, 664−673.
(41) Karickhoff, S. W.; Bailey, G. W. *Clay Miner.* **1973**, *21*, 59−70.
(42) Wang, K.; Muñoz, S.; Zhang, L.; Castro, R.; Kaifer, A. E.; Gokel, G. W. *J. Am. Chem. Soc.* **1996**, *118*, 6707−6715.
(43) Okada, Y.; Yamamoto, N.; Hayashi, T. *Bull. Chem. Soc. Jpn.* **1989**, *62*, 114−118.
(44) Bitterwolf, T. E.; Ling, A. C. *J. Organomet. Chem.* **1972**, *40*, C29−C32.
(45) Chen, Y.; Shaked, D.; Banin, A. *Clay Miner.* **1979**, *14*, 93−102.
(46) Anderson, W. L.; Stucki, J. W. *International Clay Conference*; Mortland, M. M., Farmer, V. C., Eds.; Elsevier: Amsterdam, 1979; pp 75−83.
(47) Stucki, J. W.; Golden, D. C.; Roth, C. B. *Clays Clay Miner.* **1984**, *32*, 350−356.
(48) Furukawa, T.; Brindley, G. W. *Clays Clay Miner.* **1973**, *21*, 279−288.

Received for review September 26, 2003. Revised manuscript received July 7, 2004. Accepted June 26, 2004.

ES030645+